Ecological Indicators 157 (2023) 111268

Contents lists available at ScienceDirect

Ecological Indicators

journal homepage: www.elsevier.com/locate/ecolind

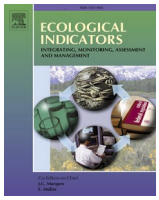

Original Articles

Vegetation-rainfall coupling as an indicator of ecosystem state in a heterogeneous landscape

Marcio B. Cure [a,*], Bernardo M. Flores [a], Caio R.C. Mattos [b,1], Rafael S. Oliveira [c], Marina Hirota [a,c,d]

[a] Graduate Program in Ecology, Universidade Federal de Santa Catarina (UFSC), Campus Universitário, s/n, Sala 208, Bloco E, Prédio Administrativo - Córrego Grande. CEP, 88040-900. Florianópolis – SC, Brazil
[b] Department of Earth and Planetary Sciences, Rutgers University. Busch Campus, 610 Taylor Rd. Piscataway, NJ 08854-8066, New Brunswick, USA
[c] Universidade Estadual de Campinas, Instituto de Biologia, Departamento de Botânica, Caixa Postal 6109, Campinas. CEP: 13083-970, Campinas, SP, Brazil
[d] Department of Physics, Universidade Federal de Santa Catarina (UFSC). Centro de Ciências Físicas e Matemáticas (CFM), Campus Universitário. Trindade. CEP, 88040-900. Florianópolis, SC, Brazil

ARTICLE INFO

Keywords:
Cerrado
Tropical vegetation
Phenology
Seasonality
Remote sensing
Ecosystem function

ABSTRACT

Coexisting vegetation types in tropical landscapes can respond in contrasting ways to rainfall, despite being in the same climatic envelope. Understanding such heterogeneity in vegetation-rainfall interactions is key for predicting how ecosystems might respond to future environmental changes. Here we test whether temporal coupling between vegetation greenness and rainfall is a good indicator of ecosystem state in the landscape. For this, we study a well-preserved landscape of the Brazilian Cerrado that is formed by mosaics of contrasting ecosystems, including savannas, dry forests and gallery forests. First, we correlate the time-series of rainfall and vegetation greenness to quantify their coupling for each vegetation type. We then compare vegetation-rainfall coupling with other state variables, such as local-scale vegetation structural and functional traits, as well as differences in environmental conditions in which these vegetation types exist. Coexisting vegetation types are set in contrasting local-scale environmental conditions and have distinct responsiveness to rainfall. Commonly used structural and functional state variables, such as tree cover and tree height, do not depict such marked differences between the vegetation types, particularly for gallery and dry forests. Dry forests have the strongest coupling and decrease their greenness during dry seasons, reflecting vegetation deciduousness on nutrient-richer soils. In contrast, gallery forests increase their greenness during the dry season, when direct radiation peaks, likely due to perennial access to groundwater. Savannas are less responsive to rainfall and have a more stable greenness throughout the year. Our findings suggest that heterogeneity in local abiotic conditions contribute to determining both vegetation distribution and ecosystem states in these tropical savanna landscapes. Changes in these conditions as a result of climate and land-use changes will likely alter the distribution of vegetation types in the future. Our functional metric may thus be useful for assessing future responses of tropical ecosystems to changes in precipitation.

1. Introduction

While precipitation plays a significant role in determining vegetation distribution at the continental or regional scale (Hirota et al., 2011; Staver et al., 2011; Maksic et al., 2022; Hély et al., 2006), landscape-scale factors, i.e. abiotic conditions, such as soil fertility (Lopes and Cox, 1977), topography (Elias et al., 2019) and fire regimes (Simon & Pennington, 2012), also contribute to determine fine scale heterogeneity in the distribution of different forests and savannas (Lehmann et al., 2014; Veenendaal et al., 2015; Bueno et al., 2018). In the Brazilian Cerrado, fine scale abiotic conditions structure vegetation mosaics with sharp boundaries, with gallery forests often occurring along the wet riparian zones and dry forests, usually dominated by deciduous tree species, on fertile soil patches (Bueno et al., 2018; Dexter et al., 2018; Pennington et al., 2018; Lira-Martins et al., 2022). Despite this high heterogeneity, large-scale studies have long considered the whole

* Correspondence author.
E-mail address: marciobcure@gmail.com (M.B. Cure).
[1] Currently at Program in Atmospheric and Oceanic Sciences, Princeton University, Princeton, NJ, USA.

https://doi.org/10.1016/j.ecolind.2023.111268
Received 11 October 2022; Received in revised form 16 October 2023; Accepted 11 November 2023
Available online 21 November 2023

Cerrado biome to be composed uniquely by savannas when using precipitation as the only predictor of vegetation distribution (e.g. Hirota et al., 2011), neglecting the concurrent role of local factors such as hydrology (e.g., Mattos et al., 2023).

For example, across the tropics, these studies consider different vegetation types, such as forests and savannas, as representing distinct ecosystem states within a range of annual rainfall totals (1000–2500 mm; Staver et al., 2011) and rainfall seasonality (less than 7 months; Staver et al., 2011). Vegetation structure, specifically tree cover, has been used as state variable to differentiate these two ecosystem types (Hirota et al., 2011; Staver et al., 2011): savannas are characterized by sparse tree cover, typically ranging from 5 % to 60 %, whereas forests exhibit a closed canopy with ~ 80 % tree cover (Hirota et al., 2011). However, it is noteworthy that using a simple structural threshold as tree cover can mask functionally different vegetation types, such as deciduous and evergreen forests (Lohbeck et al., 2013; Bueno et al., 2018; Dexter et al., 2018). While they both exhibit similar tree cover percentage when leaves are present, leaf coverage varies markedly through the year in dry forests, affecting ecosystem-level processes such as evapotranspiration and carbon assimilation (Eamus, 1999).

In this sense, the use of ecosystem functions as state variables that integrate the essence and behavior of ecosystems (Scheffer et al., 2001) is more likely to incorporate the dynamics and reveal potential responses to future environmental changes compared to structural variables alone (e.g. Berdugo et al., 2019, 2022; Maestre et al., 2016). One main terrestrial ecosystem function is primary productivity (Migliavacca et al., 2021), which is the result of the solar irradiance conversion into carbon assimilation (Monteith, 1972), thus serving as a basis to ecosystem functioning (McNaughton et al., 1989). Plant productivity is correlated with vegetation structure and climate (Michaletz et al., 2014; Migliavacca et al., 2021), and seasonal variability in productivity (i.e., phenology) depicts vegetation responses to environmental fluctuations (Alberton et al., 2019).

Satellite derived products, such as vegetation indices (e.g., EVI2, NDVI), can be used to infer gross primary productivity (GPP) and assess plant phenology and GPP dynamics spatially over broad areas (Dronova & Taddeo, 2022; Biudes et al., 2021), reflecting leaf flush (greenning) and senescence (browning) (Gao et al., 2023). Previous global analysis suggests a strong climate-biosphere coupling revealing sensitivity of ecosystems exposed to changes in precipitation regime (Lotsch et al., 2003; Alessandri & Navarra, 2008). At finer scales, responses of greenness to rainfall variability may be highly heterogeneous and depend on the vegetation type and on local environmental conditions (Chen et al., 2020).

Most studies investigating relationships between vegetation greenness and rainfall patterns have focused on large spatial scales with coarse (i.e. hundreds of meters to kilometers) data resolution (Barbosa et al., 2015; Wang et al., 2003; Davenport & Nicholson, 1993; Schmidt & Karnieli, 2000; Ichii et al., 2002; Guan et al., 2015; De Keersmaecker et al., 2017; Ayanlade et al., 2021). Such coarse spatial scale does not allow for capturing above-mentioned local scale heterogeneities in vegetation responses (Abdi et al., 2022). Furthermore, few studies focused on distinct vegetation types. For instance, Santos and Negri (1997) showed contrasting large-scale relationships between vegetation greenness and rainfall at two extremes of rainfall regimes, with a stronger correlation when rainfall is lower in Northeastern Brazil.

Understanding how distinct vegetation types respond in terms of greenness to rainfall seasonality may therefore provide insights on the underlying mechanisms driving vegetation dynamics. In this study, we test whether the coupling between vegetation greenness and rainfall can be used as a state variable (Seddon et al., 2016) capable of distinguishing between different forest and savanna types in the Brazilian Cerrado. By incorporating the temporal dimension and considering distinct forest types (dry and evergreen), we intend to gain insights into the interplay between ecological processes and their implications for ecosystem dynamics in the face of changes in precipitation (Dronova & Taddeo, 2022). We hypothesize that distinct functional ecosystem states can be differentiated at the landscape scale by the coupling between greenness and rainfall seasonality, which reflect unique vegetation strategies to cope with seasonal water deficit depending on local environmental factors.

2. Materials and methods

2.1. Study site

This study was carried out at the Chapada dos Veadeiros National Park (PNCV) (Fig. 1), located within the Cerrado biome, in Central Brazil. In 2001, the PNCV was recognized as a UNESCO World Heritage site to protect its natural and cultural areas. Currently, the PNCV protects an area of approximately 240,000 ha. We chose the PNCV for our study because its landscapes are well-preserved (i.e. without anthropic direct use) and naturally heterogeneous, with various vegetation types including savannas, riparian evergreen and gallery forests, dry forests, palm swamps, and grasslands. These vegetation types are characterized by a wide range of tree cover (Fig. 1 a-c, Fig. S1), all within the same large-scale precipitation regime, with mean annual precipitation (MAP) of around 1,500 mm/yr and a dry season from April to September (Ribeiro et al., 1983; Silva et al., 2006).

We sample a total of 30 field plots with dimensions of 20 m x 10 m totalizing an area of 200 m^2 per plot. Out of the 30 plots, 10 were located in cerrado *stricto sensu* areas (hereafter called savannas), 10 in gallery forests, and 10 in dry forests (Fig. 1). We select these vegetation types because they have been studied in the context of biome transitions (Hoffmann et al., 2012; Dexter et al., 2018). For gallery forests, we use the same control plots (i.e. six plots) of a previous study on the effects of a catastrophic fire event in the PNCV (Flores et al., 2021) and randomly select the other remaining four plots in the surrounding vegetation. For savannas, we randomly select plots between 5 % and 60 % of tree cover percentage from Hansen et al. (2013) at the spatial resolution of 30 m, according to previously defined thresholds in the context of distinct ecosystem states (Hirota et al., 2011). Dry forests are less common in the region and the most well-preserved ones are located inside private lands, within adjacent areas. Moreover, all sampled dry forests had experienced past human activities, such as logging and shelter for cattle. We randomize 10 dry forest plots within the least impacted areas of Nova Roma and Alto Paraíso de Goiás municipalities, both located within the margins of the PNCV (Fig. 1).

2.2. Environmental conditions

2.2.1. Precipitation and fire frequency data

We use monthly precipitation time series from the Climate Hazards Group InfraRed Precipitation with Station data (CHIRPS) dataset, with 0.05° spatial resolution (Funk et al., 2015) for the period between January 1981 and June 2018. We extract time series from the 30 pairs of coordinates of our sample plots and calculate the mean annual precipitation (MAP), and rainfall seasonality using the Markham Seasonality Index (MSI) (Markham, 1970) to characterize the large-scale rainfall regimes for the study area (Fig. S2). We also characterize rainfall regimes for neotropical biomes (i.e., Amazon, Cerrado, and Caatinga) to situate our sample plots along the range of values for these Biomes.

To compare precipitation regimes among the sampled vegetation types and among neotropical Biomes, we perform pairwise comparisons between factors to compute marginal means and confidence intervals for each combination of factors. Subsequently, we conduct multiple comparison tests to identify significant differences between groups (or not) by comparing all factor levels, such as biomes and vegetation types. Analysis was performed with the R package *emmeans* (Lenth, 2022).

In addition, we use MapBiomas Fire Collection 1 (Alencar et al., 2022) to obtain fire frequency data from 1985 to 2018 with 30 m resolution extracted from the plot coordinates to characterize fire regimes

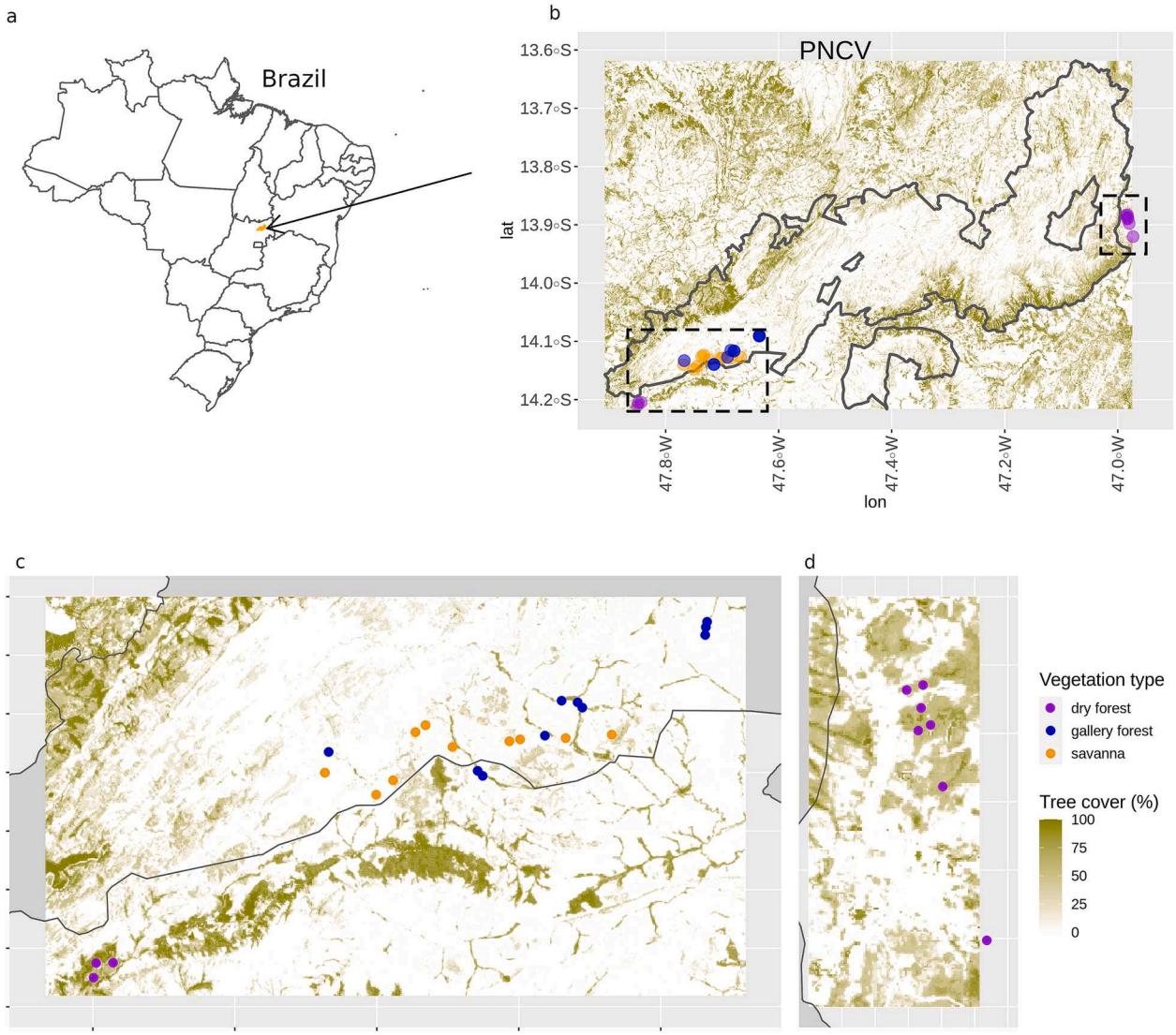

Fig. 1. In (a), Brazilian map with the arrow pointing to the Chapada dos Veadeiros National Park (PNCV) highlighted in orange. In (b), the PNCV is limited by a gray line and shows tree cover according to the legend. Dotted squares are zoomed in (c) and (d). Our sample plots are shown in circles with each color representing different vegetation types as described by the legend. (c) and (d): zooming in our sample plots showing the position of each plot in relation to the PNCV borders. Note that dry forests (purple dots) are outside the PNCV.

for the different vegetation types (Projeto Mapbiomas; Souza et al., 2020).

2.2.2. Soil samples

We collect three superficial soil samples (0——20 cm) well spaced in each plot to represent local soil characteristics. Samples were analyzed at the Soil Department Laboratory of the Universidade Federal de Viçosa, Brazil, for the following: effective cation exchange capacity (t), sum of bases (SB), soil pH, aluminum (Al3 +), iron (Fe), potential acidity, base saturation index (V), aluminum saturation index (m), soil texture and available nutrients [i.e., total phosphorus (P), calcium (Ca2 +), nitrogen (N), potassium (K), copper (Cu), zinc (Zn), magnesium (Mg2 +) and manganese (Mn)]. pH was extracted with H2O; remaining phosphorus (P-Rem), potassium (K), iron (Fe), zinc (Zn), manganese (Mn) and copper (Cu) with Mehlich-1; calcium (Ca2 +), magnesium (Mg2 +) and aluminum (Al3 +) with KCl 1 mol/L. The colorimetric method (ascorbic acid) was used to determine P; flame emission spectrometer for K, Na, Fe, Mn, Zn and Cu; atomic absorption spectrometer for Ca2 + and Mg2+; titration with bromothymol blue and NaOH for Al3 +.

Using all soil variables, we perform a Principal Component Analysis (PCA) based on Euclidean distances of the standardized variables to simplify part of the variance of several soil attributes, using the 'decostand' and 'rda' functions from the 'vegan' package (Oksanen et al., 2020) and the 'prcomp' function from the 'stats' package in the R Software for Statistical Computing (R Core Team, 2021). To understand how samples are grouped by similarity regarding soil attributes, we used the Ward's minimum variance method (Murtagh & Legendre, 2014) to clusterize sample plots by Euclidean distances of their soil characteristics using both 'dist' and 'hclust' functions from the 'stats' package.

2.2.3. Topographic Wetness Index (TWI): Water in the soil

To characterize plant water access conditions, we use the Topographic Wetness Index (TWI) as a proxy for water availability from each plot coordinate. The TWI (Beven & Kirkby, 1979) has long been used on hydrological studies (e.g., Western et al., 1999) as a proxy for soil moisture, and more recently has been applied to ecological studies to explain the distribution of vegetation along topographic gradients (Alexander et al., 2016; Moeslund et al., 2013). The TWI is defined as ln (A/tan β), where A is the specific catchment area above a certain point in

the terrain and β is the terrain slope. Larger TWI values are associated with lower convergent areas where water tends to accumulate and soil moisture availability is high. We calculate the TWI using the GRASS package on the open-source QGIS software, using the MERIT-Hydro Digital Elevation Model (90 m resolution) as the basis for our calculations (Yamazaki et al., 2019). We note that this is a first-order estimate of soil water conditions, based only on topography, and does not account for factors such as difference in soil properties and local geology. Despite these limitations, the TWI has been shown to be useful in differentiating hydrologic environments (e.g., drier uplands vs wetter lowlands) and their effect on vegetation distribution and structure (Metzen et al., 2019; El-Hokayem et al., 2023; Alexander et al., 2016).

2.3. Ecosystem state variables

2.3.1. Tree community structure and functional traits

We chose 4 structural and functional traits to serve as ecosystem state variables (i.e. variables characterizing the ecosystem) and to test their performance in relation to the coupling: tree height, bark thickness, tree basal area and deciduousness. Trees were selected depending on the vegetation type: for forests, we selected individuals with diameter at breast height greater or equal than 10 cm (DBH $\geq$ 10 cm); while for savannas, we sampled trees when the DBH was greater or equal than 3 cm, i.e., with lower DBH than forest individuals (Maracahipes et al., 2018). We defined such sampling design to ensure the effective representation of the total basal area of woody vegetation in both forest and savanna ecosystems.

We sample tree height because it has already been used to characterize distinct vegetation types (Xu et al., 2016) and because it is an indicator of several ecosystem functions. For example, tree height is related to resource availability, respiration, hydraulic traits and also to aboveground biomass (Liu et al., 2019; McDowell et al., 2002; Ryan & Yoder, 1997). We also measure bark thickness given its role in determining vegetation structure and function related to fire regimes (Bernardino et al., 2022; Dantas et al., 2016; Lawes et al., 2011; Pausas and Poorter, 2015). Moreover, bark thickness has been reported to have multiple additional functions, such as protection against herbivores, storage of water and other compounds, photosynthetic activity and mechanical support (Rosell, 2019). This trait was measured using the bark gauge MAC-100 by Haglöf Sweden and relativized using tree basal area (Lawes et al., 2013). Although relative bark thickness has not been used in the literature as a state variable so far, it can clearly separate forest and savanna states (Bernardino et al., 2022; Dantas et al., 2016). To characterize tree communities of each plot, we calculate the community mean for tree height and relative bark thickness.

Another ecosystem state variable selected was the tree basal area (TBA). TBA is an indicator of aboveground biomass, nutrient availability and soil physical characteristics (Emilio et al., 2014; Rozendaal et al., 2020; Slik et al., 2010) and has been used as a state variable describing vegetation structure (Dantas et al., 2016). It is calculated as the sum of areas of tree trunks and scaled to one hectare. We computed the trunk areas based on DBH.

We calculate community-level deciduousness as the difference between wet and dry season tree cover measured in the field, as an indicator of changes in green leaf area. Wet and dry season measures were taken in April and September respectively. We were unable to measure deciduousness for 5 dry forest plots, for 2 gallery forest plots and for 2 savanna plots due to vegetation burning and cutting between the measurements. Deciduousness can be used as an integrative indicator of vegetation functioning, depending on water and nutrient availability (Oliveira et al., 2021).

In addition to plot sampling (see above in section 2.1), we use satellite-derived tree cover measurements (Hansen et al., 2013) to compare with our tree cover percentage measured in the field. We estimate tree cover for our plots (i.e., at the community scale) as the mean of 16 measurements for each plot, with four measurements at each corner (facing North, South, East and West), using a convex densiometer. For our 30 sample plots, the *in situ* densiometer-derived tree cover and the remotely-sensed estimated tree cover are strongly correlated ($\rho = 0.84$, $t = 7.57$, $p < 0.05$), but satellite data tend to overestimate savanna coverage, while underestimating forest tree cover (Fig. S1). Although such mismatches might not make a substantial difference in large-scale analyses (e.g., Hirota et al., 2011; Staver et al., 2011), here, 12 out of our 20 forest plots would not be classified as forests using satellite data. The densiometer-derived tree cover represents vegetation type structure with more precision by capturing the fine scale structure (Fig. S1b). Hence, we choose to use field densiometer-derived tree cover as our metrics for tree cover at the community level. The relationship between structural/functional state variables (e.g., tree height, basal area, bark thickness) and tree cover has been used to test if functional alternative states correspond to structural ones (e.g., Bernardino et al., 2022; Dantas et al., 2016; Xu et al., 2016).

2.3.2. Satellite EVI2 data for vegetation greenness

As a proxy for vegetation greenness (Biudes et al., 2021), we use the 2-band Enhanced Vegetation Index (EVI2) from Landsat 8 (OLI), at 30 m spatial resolution, available for the period between April 2013 to June 2018. EVI2 is calculated based on both red (Band 4) and near infrared (Band 5) bands. These bands represent fractions of the electromagnetic spectrum (640–1400 nm) that correspond to photosynthetic radiation reflected and absorbed by plant leaves, respectively, thus indicating vegetation greenness; in particular with new green leaves exposed to sunlight. We computed the EVI2 using the formula:

$$EVI2 = 2.5 \times (band\ 5 - band\ 4)/(band\ 5 + 2.4 \times (band\ 4) + 1)$$

EVI2 was developed to have the efficiency of Enhanced Vegetation Index (EVI) and to avoid saturation at high vegetation biomass, while minimizing soil and atmosphere influences without the blue band (Jiang et al., 2008), i.e., to improve the representation of greenness heterogeneity in forest ecosystems. We extract the 16-day values for each sample plot and calculate the mean EVI2 for each month, as well as standard deviation, maximum values and amplitude. We excluded time series values that have a quality flag indicating cloud cover. Given the temporal resolution of 16 days in which Landsat 8 acquires the images used, all time series have between 1 % and 4 % of their values contaminated by clouds. Such contamination was not a major concern because we were able to ensure at least one cloud-free value per month. This suggests that despite cloud cover, there was sufficient data available for analysis in each month.

We calculate mean, maximum and standard deviation in EVI2 for each plot to additionally serve as functional state variables.

2.3.3. Coupling between precipitation and greenness

We propose to use the coupling between EVI2 and rainfall as a state variable that comprises the temporal dynamics of vegetation response to rainfall fluctuations. The coupling between the monthly time series of precipitation and EVI2 for each plot is computed using the Kendall cross-correlation coefficient (*tau*). Positive *tau* values indicate that vegetation is in phase with precipitation (EVI2 changes together with precipitation), whereas negative values indicate the opposite (EVI2 follows an opposite direction of precipitation changes). Additionally to the calculation of the coupling, we also perform a cross-correlation analysis that results in values of maximum coupling and associated lag (moving precipitation from 0 to 6 months backward to be correlated with the current EVI2). Finally, we also considered the maximum coupling as a functional state variable to differentiate vegetation types. A flowchart illustrating the step-by-step process for deriving the biotic and abiotic variables is provided in Figure S13.

We utilized statistical tests to differentiate between vegetation types based on the EVI2 signal, which indicates vegetation greenness behavior, as well as state variables that describe vegetation functioning, structure, and environmental conditions. We use the Mann-Kendall

trend test from the Kendall package (McLeod, 2011) to assess trends in monthly median EVI2 values during the dry season months. This analysis aids in highlighting differences in vegetation behavior during the drier months and may also reveal the impact of rainfall-water stress on greenness direction. Furthermore, we conducted a Mann-Whitney *U* test (Sijtsma & Emons, 2010) to compare pairs of different vegetation types across various attributes, including maximum coupling, lag, tree height, total basal area, relative bark thickness, deciduousness (changes in tree cover), TWI, fire frequency, soil variables and PCA derived axis between pairs of different vegetation types, using the R package 'stats' (R Core Team, 2021). We also set the *alternative* argument in the *wilcox.test* function to either *less* or *greater* to test the hypothesis that values of one vegetation type are lower or greater, respectively, than values of the other vegetation type. Analyses and data manipulation were performed in R version 4.1 (R Core Team, 2021).

3. Results

3.1. Heterogeneity in environmental conditions

Gallery forests and savannas are embedded within the same rainfall regime (both mean annual precipitation, MAP, and seasonality), whereas dry forests are set under a statistically different mean annual precipitation (Fig. S2). Despite differences shown in the analysis of MAP for dry forests, the values are very close compared with the range of values for the Cerrado biome (Fig. S2a). Furthermore, all vegetation types are inside the bistability zone for MAP defined by Staver et al. (2011), i.e. they exist within a rainfall envelope that supports both forests and savannas. At finer scales, however, savannas, gallery forests and dry forests occur in distinct environmental conditions regarding water access, soil characteristics and fire frequency (Fig. 2, Figs. S3-6; Fig. S7; Table S1). First, soil moisture availability is higher in gallery forests followed by savannas and dry forests (Fig. 2; Tables S1 and S2; Figs. S6-d).

Secondly, regarding soil characteristics, gallery forests have higher amounts of Ca, Mg, N, total P, K, Zn, Mn, sum of bases, and cation exchange capacity than savannas (Table S3). Nevertheless, they are more similar to savannas than to dry forests (Fig. S4b; Table S1), as shown by their overlap in the PC1 (Fig. 2-a, Fig. S4 a; Table S1). PC1 explains more than 63.85 % of soil variance and is positively correlated with base saturation index, Mg2, sum of bases, Ca2, t, Mn, pH and K; PC1 is also negatively correlated with Aluminum saturation index, exchangeable Aluminum and potential acidity (Fig. S4; Table S3). PC2 explains 19.13 % of soil variance and is more related to total N, effective cation exchange capacity, potential acidity, Fe, and P; it also separates all vegetation types (Tables S1 and S3; Figs. S4 and S7b). Except for N, Fe and total P, overall concentrations of soil nutrients in the dry forests are higher than in gallery forests and savannas (Fig. S3-4 and S6a-b; Table S4). Despite the similarities in PC1, gallery forests and savannas have well pronounced differences (Fig. S7a) such as higher amounts of N and P and lower sand content in gallery forests (Table S4; Figs. S3-5). Gallery forests and savannas are present within more acidic soils if compared to dry forests (Table S4), while dry forests are related to more fertile soils with higher cation exchange capacity (positive values in the

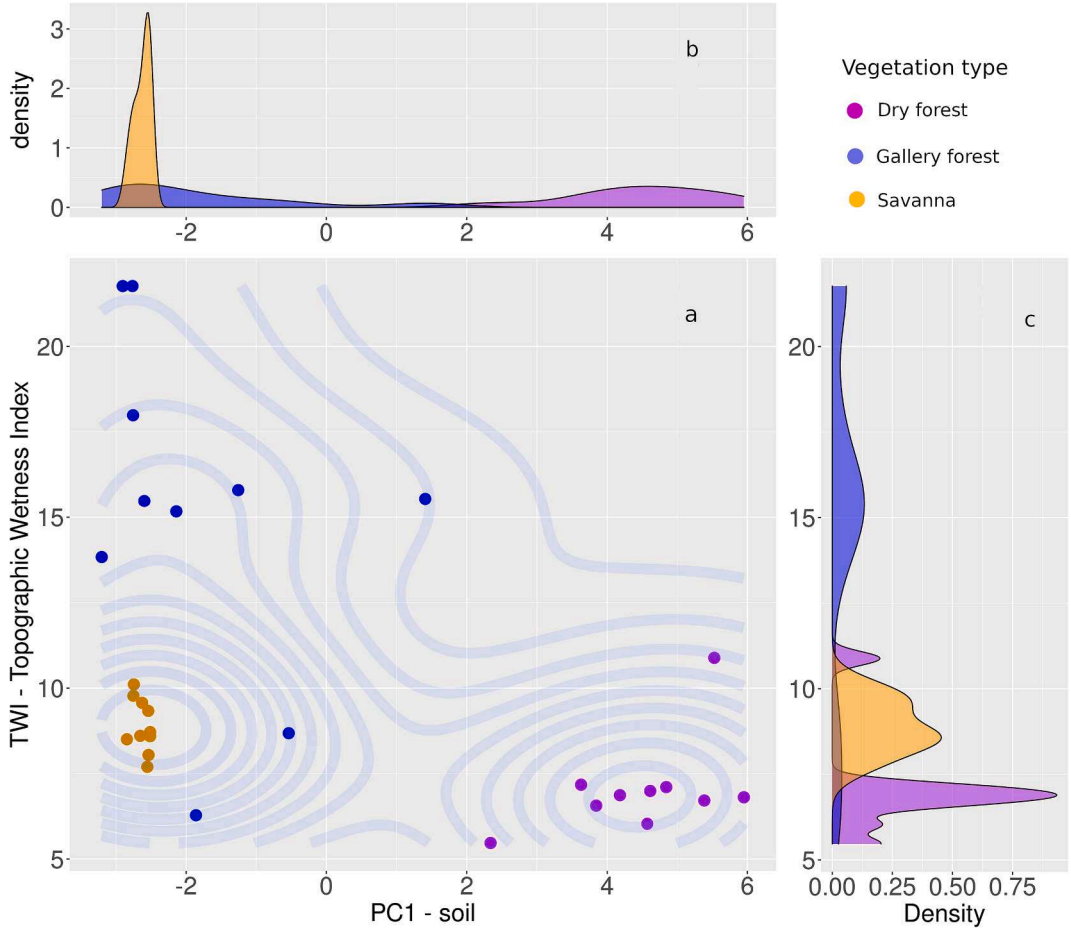

Fig. 2. Three coexisting vegetation types within a two-dimensional space of environmental conditions. a) The main panel shows the density distribution of environmental conditions (vertical axis: TWI; horizontal axis: soil first principal component) represented in a plane for the different vegetation types at the Chapada dos Veadeiros National Park. b) Density distribution of the PC1 of soil variables shows overlap of soil conditions for gallery forests and savannas, while dry forests are distinct from the rest. c) TWI separates gallery forests from savannas, but overlaps occur for savannas and dry forests in one case, as well as for gallery and dry forests.

PC1; Table S4) without exchangeable aluminum (Fig. S3-4).

Fire frequency differs between vegetation types (Fig. S6; Fig. S7b; Table S1), with savannas more frequently affected by fire than both forest types for the study period (Table S2). Forest types also differ in fire frequency: while only one dry forest plot burned (twice) in the 33 years, gallery forests burned on average 2.9 times (Table S2). Thus, our results show that fire events occur in gallery forests (less frequent) and savannas (more frequent) (Table S2), but rarely in dry forests.

3.2. Ecosystem state variables

The maximum coupling reveals substantial differences among vegetation types (Fig. 3a, Figs. S8-10; Table S3; Fig. S7c). Dry forests present the largest positive maximum coupling (Table S6; median *tau* = 0.4), indicating that greening follows the increase in rainfall amounts during the wet season (Figs. S11b,e and S12c). On the other hand, gallery forests have the largest negative maximum coupling, indicating that greening occurs before the start of the wet season (median *tau* = -0.27), more specifically, with a peak at the end of the dry season (Figs. S11c,f and S12b). Savannas have a small maximum coupling (median *tau* = 0.18, Fig. S12a), with the least variation (Table S6) in EVI2 (mean standard deviation = 0.16; Fig. 3a,b and S11d,g). All vegetation types have significant differences among their distributions of coupling (Table S5; Fig. S7c), with little overlap (Fig. 3a). Moreover, different vegetation types respond to precipitation with different lags for the strongest response: gallery forests are the fastest (lag in response of 0 to 1 month), while dry forests respond within 1–2 months and savannas have a mean lag of 2.8 months (Fig. S7c; Tables S5 and S6).

Savannas are the most stable in terms of greenness fluctuations (EVI2 standard deviation = 0.02), and present the lowest mean values (mean = 0.37) (Fig. 3b, Fig. S11e-g; Table S5). EVI2 means and variations in dry and gallery forests are similar (Fig. 3b; Fig. S7c; Table S4), but the annual cycle is different in terms of the time greening occurs (Figs. S11-S12). During the dry season, gallery forests have a positive trend (*tau* = 0.867, $p < 0.05$), i.e., an increase in greenness before rainfall starts (Figs. S11c,f and S12b), dry forests have a negative trend (*tau* = -1, $p < 0.05$), indicating a decline in canopy greenness (Figs. S11b,e and S12b, c). Savannas are fairly insensitive to rainfall variation (*tau* = -0.6, $p > 0.05$) and maintain a stable EVI2 throughout the dry season (Figs. S11d, g and S12a).

In terms of deciduousness, gallery forests and savannas are similar (Fig. S7c; Table S5), characterized by relatively small increases in the percentage of green leaf area (gallery forest: mean = -1.43, sd = 4.94; savanna: mean = -7.3, sd = 10.02) during the dry season, while dry forests present a pronounced decrease (mean = 49.67, sd = 8.43) (Fig. 3c).

Gallery and dry forests are clearly differentiated from savannas, with higher values in tree height and TBA for both forest types (Fig. 3d-e; Table S5; Table S6; Fig. S7b). Gallery forests have the highest TBA followed by dry forests and savannas (Fig. 3e; Table S6). Furthermore, savannas have a higher relative bark thickness in comparison with both types of forests (Table S6), and dry forests have a higher relative bark thickness than gallery forests (Table S6; Fig. 3f).

The three vegetation types can be clearly distinguished when viewed in the tree cover-coupling and tree cover-deciduousness two-dimensional spaces (Fig. 4a, c). However, only coupling is able to separate all three vegetation types when considered as a single state variable (Fig. 4; Fig. S7; Table S5), whereas deciduousness alone cannot separate between gallery forests and savannas (Fig. S7; Table S5). Moreover, only forests (both types) and savannas appear as separate states when tree cover is combined with mean EVI2, tree height, TBA and relative bark thickness, missing the distinction between dry and gallery forests (Fig. 4b, d-f).

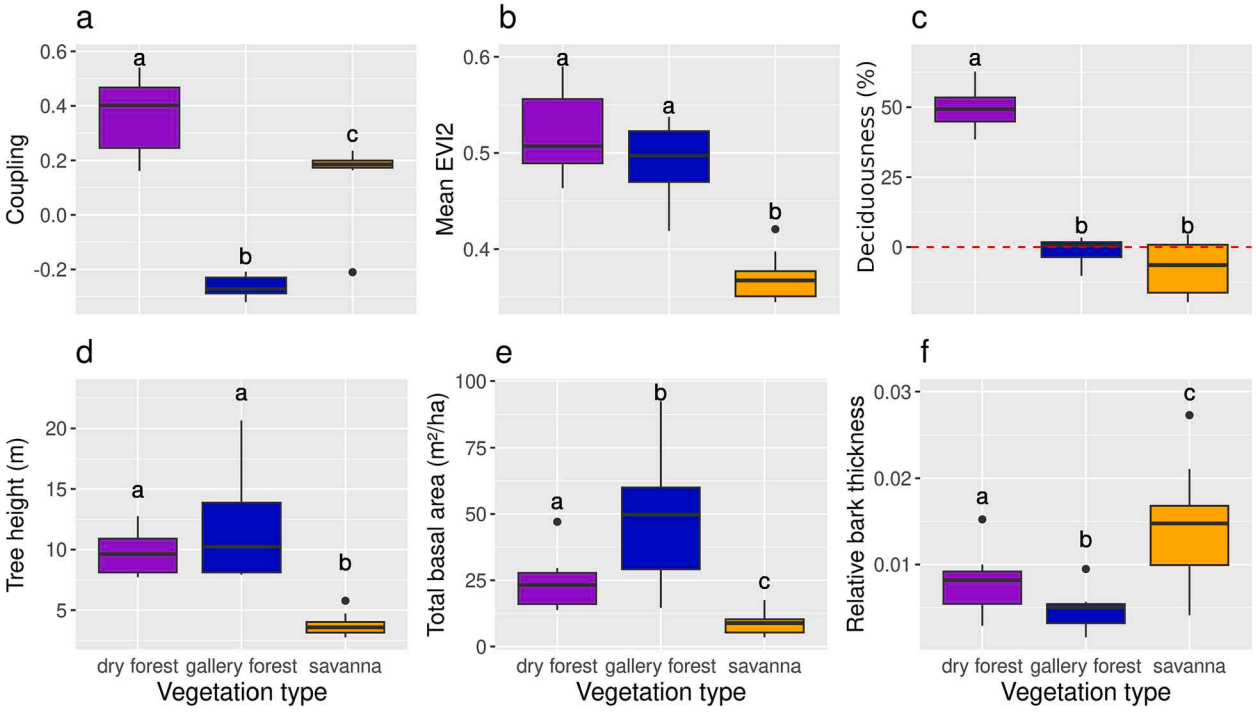

Fig. 3. Functional state variables used in this study to highlight differences and similarities among vegetation types in the Chapada dos Veadeiros National Park (PNCV), Brazil. (a) Coupling between 2-band Enhanced vegetation Index (EVI2) and precipitation. Note that the magnitude of the coupling is indicated by the absolute value of the maximum coupling with lag between monthly EVI2 and precipitation; (b) Mean values of EVI2; (c) Deciduousness: green leaf area changes (positive values, loss or gain, negative values) from the wet to the dry season as evidence of growth for savanna and gallery forest during the dry season. Negative values mean increase in tree cover while positive values mean decrease in tree cover.; (d) Tree height; (e) Total basal area per hectare; and (f) Bark thickness relative to tree basal area for dry forests, gallery forests and savannas. Letters above each box indicate the differences and similarities between vegetation types based on Mann-Whitney U tests, with p-value < 0.05.

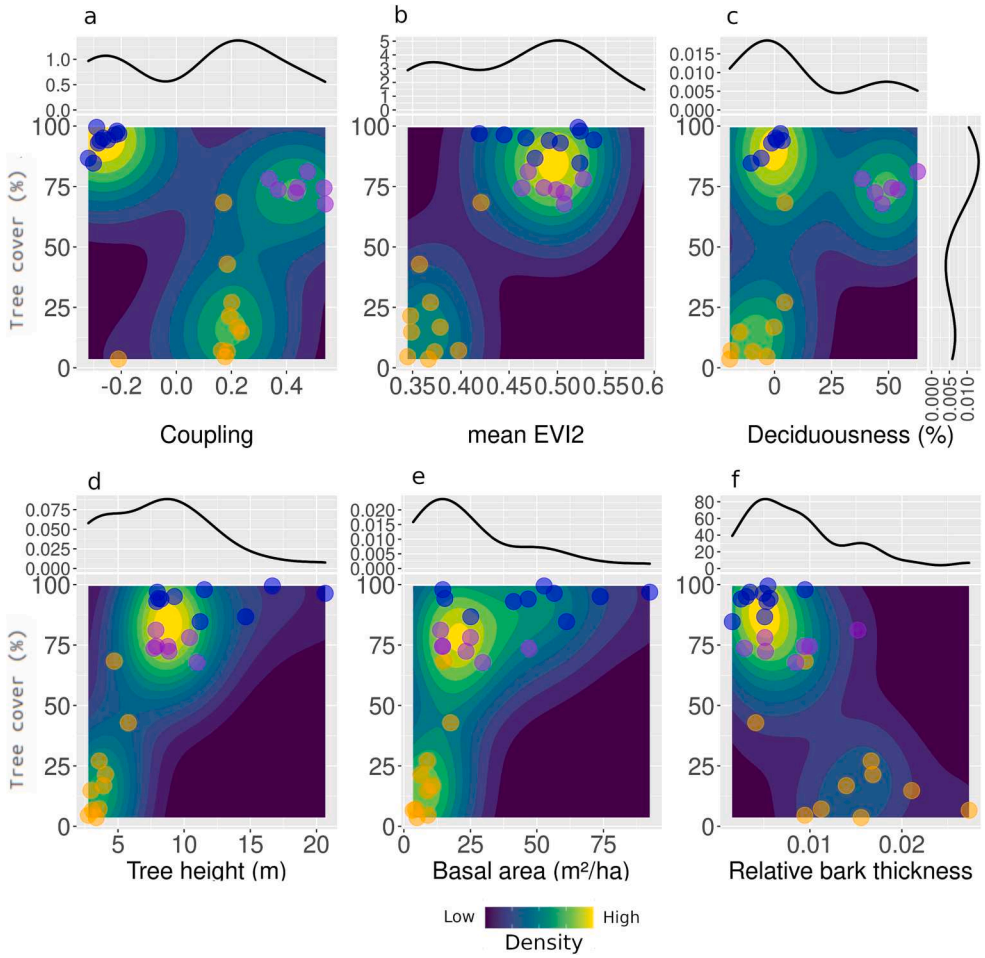

Fig. 4. Relations between state variables with tree cover to test for correspondence between functioning and structure. The color gradient in panels represent density distribution of plots (low density – marine blue; high density - yellow). Orange dots are savannas, purple dots are dry forests, and blue dots are gallery forests. (a) Maximum coupling; (b) mean EVI2; (c) deciduousness derived from the difference between percentages of tree covers in the end of the wet season and in the end of the dry season; (d) tree height (m); (e) total basal area per hectare (m^2/ha); and (f) Relative bark thickness (bark thickness divided by tree basal area).

4. Discussion

Our findings suggest that the greenness-rainfall coupling can be a novel and mechanistic way of differentiating between coexisting vegetation types in the same rainfall envelope (Fig. 4). This ecosystem-level functional variable shines new light on tropical landscape heterogeneity (Turner & Chapin, 2005), separating dry and gallery forests that were previously indistinguishable using the satellite-derived tree cover data (e.g. Hirota et al., 2011). Other structural/functional variables previously used to characterize alternative stable states (Xu et al., 2016; Dantas et al., 2016; Bernardino et al., 2022), such as tree height, TBA, and relative bark thickness also failed in differentiating between forest types. Even with distinct TBA and relative bark thickness, gallery and dry forests are still in the same attractor of forests (see Table 1 from Dantas et al., 2016; and Fig. 2 from Bernardino et al., 2022). Although deciduousness has been proposed by an integrative variable to define strategies to deal with droughts (Oliveira et al., 2021), it did not differentiate gallery forests and savannas (Figs. 3 and 4; Table S5). Our results thus indicate that the temporal dynamics of vegetation responses to rainfall provides a more meaningful indicator (i.e. a functional one) for characterizing distinct ecosystems in the landscape than simple structural variables (Dronova & Taddeo, 2022).

Our results show that gallery forests, dry forests and savannas coexist in the same landscape under different conditions of soil nutrients and water accessibility (Ratter & Dargie, 1992; Oliveira & Marquis, 2002; Ribeiro & Walter, 2008; Cowling & Potts, 2015; Lira-Martins et al., 2022) (Fig. 2; Fig. S3; Fig. S5; Fig. S6 a-c; Fig. S7a-b), suggesting they may not be alternative stable states after all (Veenendaal et al., 2015). Fire regimes could be another explanation for the distribution of forests and savannas in this landscape (Hoffmann et al., 2012; van Nes et al., 2018), but our analyses also suggest that they might play a smaller role, compared to soil conditions (Veenendaal et al., 2015). Soil conditions shape the variety of strategies to cope with the strong water deficit experienced by all vegetation types during the dry season and the consequent response each vegetation type presents to rainfall seasonal variation (Oliveira et al., 2021). For instance, savannas invest primarily on deep roots to access water and build a drought resistant xylem (Oliveira et al., 2005; Scholz et al., 2008; Loram-Lourenço et al., 2022; Jancoski et al., 2022). As a result, we observe a high stability in greenness and consequent weak coupling, particularly because all plots have significant woody tree strata (mean = 62 %, sd = 35). Annual C_4 herbaceous species tend to be highly coupled with rainfall and thus more variable (Ma et al., 2020; Whitecross et al., 2017), whereas savanna trees with deep roots may contribute to a lower variability in water availability, and consequently in ecosystem greenness (Lee et al., 2021; Oliveira et al., 2005; Priyadarshini et al., 2016).

Biogeographical and evolutionary processes may have contributed to make savannas in the Cerrado (a tropical savanna biome) more diverse in strategies to deal with their environment (Simon et al., 2009), compared to evergreen and deciduous forests that occupy smaller areas within the savanna landscape (Projeto Mapbiomas, 2022). One hypothesis is that higher diversity of plant strategies may have contributed

to increasing savanna greenness stability to rainfall fluctuations (Liang et al., 2016; Oehri et al., 2017). A similar pattern was observed in the dry forests of the Caatinga biome, where areas with higher phylogenetic diversity had higher greenness stability than areas with lower diversity (Mazzochini et al., 2019).

The dominant ecological strategy in dry forests for dealing with seasonal drought relies on deciduousness to avoid water losses and possible hydraulic system collapse (Castro et al., 2018; Cuba et al., 2018; Oliveira et al., 2021). With high nutrient availability, trees lose their leaves because they can easily grow new leaves before the next rainy season (Sobrado, 1991; Kikuzawa, 1995). Indeed, dry forest soils in our study landscape had a higher cation exchange capacity and low exchangeable aluminum content than gallery forests and savannas and this is likely determined by geomorphic processes not by feedback with vegetation (Dexter et al., 2018; Lira-Martins et al., 2022; Paula et al., 2023). The new leaves produced by the tree community every year may thus contribute to boost greening during the rainy season (Mazzochini et al., 2019). This way, dry forests exhibit greenness closely following rainfall seasonal variations, with a significant decrease during the dry season (Fig. S11), reflected in their EVI2 signal (Goldstein et al., 1989; Eamus, 1999; Ishida et al., 2006; de Souza et al., 2020).

Gallery forests were the only vegetation type showing increased greenness during the dry season and thus a negative coupling with rainfall (Fig. 3a, Figs. S11-12). One possible explanation is that gallery forests have perennial access to groundwater (Veneklaas et al., 2005; Bueno et al., 2018), i.e., they are not water-limited (Green et al., 2020; Smith et al., 2020). Increased greening is likely a result of dry-season leaf flushing, which allows trees to attain higher photosynthetic activity in a period of lower cloud cover and increased radiation (Saleska et al., 2007). Similar to our sampled gallery forests, Amazonian forests reach peak greenness during the dry season, when cloud cover is low and incoming radiation is high (Guan et al., 2015).

Contrary to the well reported fire-vegetation feedback maintaining savannas and forests as alternative stable states (Bernardino et al., 2022; Bond et al., 2005; Dantas et al., 2016; Hoffmann et al., 2012; Murphy & Bowman, 2012; Pausas & Bond, 2021; Staver et al., 2011), we found that gallery forests have higher fire frequency than previously reported (Ribeiro & Walter, 2008). Even with the highest tree cover and moisture availability, all gallery forests experienced at least one fire event between 1985 and 2018 (mean = 2.9 fires), while only one dry forest plot burned in this period (Fig. S6c). Dry forests likely burnt from fires ignited to expand the surrounding pastures for cattle. Gallery forests are narrow and surrounded by flammable savannas, from where such fires may spread into the forest (Ribeiro & Walter, 2008; Kellman and Meave, 1997). Nonetheless, gallery forests may suffer mild burns and still keep high tree cover under a long fire return interval, likely because fire events may not be strong enough to open the forest canopy (Veenendaal et al., 2018). Strong widespread fires, however, may severely impact the ecosystem, killing most trees and destroying the organic soil layer (Flores et al., 2021).

5. Conclusion

We have shown how the temporal coupling between greenness and precipitation inferred from satellite can be an integrative state variable and a promising ecological indicator for broad-scale analyses differentiating between coexisting vegetation types. Our coupling measure reveals that savannas, gallery forests and dry forests at the same landscape have distinct responses in terms of greenness to rainfall seasonality partially determined by nutrient and water availability at the local scale. Our results have also shown that vegetation with similar structure (i.e. gallery and dry forests) may have contrasting functioning and responses to rainfall variability. Combined, these results suggest that presuming the absence of feedback mechanisms (Staal and Flores, 2015), coexisting vegetation types may not necessarily be alternative stable states (Hirota et al., 2011; Staver et al., 2011), since their distribution is strongly determined by fine scale heterogeneity in environmental conditions.

Authors' Contributions:

MBC, BMF, RSO and MH conceived the idea. MBC and BMF collected the data. MBC analyzed data and CRCM calculated TWI. MBC wrote the first draft of the manuscript and all others contributed to the final version.

Data Availability Statement

Study data, plot coordinates, and detailed methods and outputs on the rainfall analysis are available at https://github.com/Mauritia-flexuosa/Cure-et-al-pncv-data. Satellite data was downloaded from Earth Explorer at www.earthexplorer.usgs.gov, precipitation data from CHIRPS at https://data.chc.ucsb.edu/products/CHIRPS-2.0/, and fire frequency from Projeto Mapbiomas at https://code.earthengine.google.com/?scriptPath = users%2Fmapbiomas%2Fuser-toolkit%3Amapbiomas-user-toolkit-fire.js.

Declaration of Competing Interest

The authors declare that they have no known competing financial interests or personal relationships that could have appeared to influence the work reported in this paper.

Data availability

I have shared the link to my data/code at the mauscript.

Acknowledgments

MBC thanks the Fundação de Amparo à Pesquisa e Inovação do Estado de Santa Catarina (FAPESC) for scholarship, the Fundo Brasileiro para a Biodiversidade (FUNBIO) and the Instituto da Humanidade (Humanize) for financing field trips, and the Instituto Serrapilheira (grant number Serra-1709-18983) for financing soil analysis and contributing to data collection. BMF and MH are supported by Instituto Serrapilheira (Serra-1709-18983). RSO received a CNPq productivity scholarship. We also thank Isabel Schmidt, Alexandre Sampaio, Caroline Camargo, Lauro Jurgeaitis, Ângelo Testa, the Instituto Chico Mendes de Conservação da Biodiversidade (ICMBio), and the Secretaria do Estado de Meio Ambiente e Desenvolvimento Sustentável (SEMAD Goiás) for facilitating our work. We would also like to thank friends and colleagues for fundamental help during field trips and insightful discussions.

Appendix A. Supplementary data

Supplementary data to this article can be found online at https://doi.org/10.1016/j.ecolind.2023.111268.

References

Abdi, A.M., Brandt, M., Abel, C., Fensholt, R., 2022. Satellite remote sensing of savannas: current status and emerging opportunities. J Remote Sens 2022.

Alberton, B., da Silva Torres, R., Sanna Freire Silva, T., Rocha, H., S. B. Moura, M., Morellato, L., 2019. Leafing patterns and drivers across seasonally dry tropical communities. Remote Sens. (Basel) 11 (19), 2267.

Alencar, A.A.C., Arruda, V.L.S., Silva, W.V.d., Conciani, D.E., Costa, D.P., Crusco, N., Duverger, S.G., Ferreira, N.C., Franca-Rocha, W., Hasenack, H., Martenexen, L.F.M., Piontekowski, V.J., Ribeiro, N.V., Rosa, E.R., Rosa, M.R., dos Santos, S.M.B., Shimbo, J.Z., Vélez-Martin, E., 2022. Long-term landsat-based monthly burned area dataset for the brazilian biomes using deep learning. Remote Sens. (Basel) 14 (11), 2510.

Alessandri, A., Navarra, A., 2008. On the coupling between vegetation and rainfall interannual anomalies: Possible contributions to seasonal rainfall predictability over land areas. Geophys. Res. Lett. 35, L02718. https://doi.org/10.1029/2007GL032415.

Alexander, C., Deák, B., Heilmeier, H., 2016. Micro-topography driven vegetation patterns in open mosaic landscapes. Ecol. Ind. 60, 906–920. https://doi.org/10.1016/j.ecolind.2015.08.030.

Ayanlade, A., Jeje, O.D., Nwaezeigwe, J.O., Orimoogunje, O.O.I., Olokeogun, O.S., 2021. Rainfall seasonality effects on vegetation greenness in different ecological zones. Environmental Challenges 4, 100144. https://doi.org/10.1016/j.envc.2021.100144.

Barbosa, H.A., Lakshmi Kumar, T.V., Silva, L.R.M., 2015. Recent trends in vegetation dynamics in the South America and their relationship to rainfall. Nat. Hazards 77, 883–899. https://doi.org/10.1007/s11069-015-1635-8.

Berdugo, M., Maestre, F.T., Kéfi, S., Gross, N., Le Bagousse-Pinguet, Y., Soliveres, S., Gomez-Aparicio, L., 2019. Aridity preferences alter the relative importance of abiotic and biotic drivers on plant species abundance in global drylands. J. Ecol. 107 (1), 190–202.

Berdugo, M., Vidiella, B., Solé, R.V., Maestre, F.T., 2022. Ecological mechanisms underlying aridity thresholds in global drylands. Funct. Ecol. 36 (1), 4–23. https://doi.org/10.1111/1365-2435.13962.

Bernardino, P.N., Dantas, V.L., Hirota, M., Pausas, J.G., Oliveira, R.S., 2022. Savanna-forest coexistence across a fire gradient. Ecosystems 25 (2), 279–290.

Beven, K.J., Kirkby, M.J., 1979. A physically based, variable contributing area model of basin hydrology/Un modèle à base physique de zone d'appel variable de l'hydrologie du bassin versant. Hydrol. Sci. Bull. 24 (1), 43–69. https://doi.org/10.1080/02626667909491834.

Biudes, M.S., Vourlitis, G.L., Velasque, M.C.S., Machado, N.G., de Morais Danelichen, V. H., Pavão, V.M., Arruda, P.H.Z., de Souza Nogueira, J., 2021. Gross primary productivity of Brazilian Savanna (Cerrado) estimated by different remote sensing-based models. Agric. For. Meteorol. 307, 108456 https://doi.org/10.1016/j.agrformet.2021.108456.

Bond, W.J., Woodward, F.I., Midgley, G.F., 2005. The global distribution of ecosystems in a world without fire. New Phytol. 165 (2), 525–538. https://doi.org/10.1111/j.1469-8137.2004.01252.x.

Bueno, M.L., Dexter, K.G., Pennington, R.T., Pontara, V., Neves, D.M., Ratter, J.A., de Oliveira-Filho, A.T., Durigan, G., 2018. The environmental triangle of the Cerrado Domain: Ecological factors driving shifts in tree species composition between forests and savannas. J. Ecol. 106 (5), 2109–2120.

Castro, S.M., Sanchez-Azofeifa, G.A., Sato, H., 2018. Effect of drought on productivity in a Costa Rican tropical dry forest. Environ. Res. Lett. 13 (4), 045001 https://doi.org/10.1088/1748-9326/AAACBC.

Chen, Z., Wang, W., Fu, J., 2020. Vegetation response to precipitation anomalies under different climatic and biogeographical conditions in China. Sci. Rep. 10 (1), 1–16. https://doi.org/10.1038/s41598-020-57910-1.

Cowling, R.M., Potts, A.J., 2015. Climatic, edaphic and fire regime determinants of biome boundaries in the eastern Cape Floristic Region. S. Afr. J. Bot. 101, 73–81. https://doi.org/10.1016/J.SAJB.2015.03.182.

Cuba, N., Lawrence, D., Rogan, J., Williams, C.A., 2018. Local variability in the timing and intensity of tropical dry forest deciduousness is explained by differences in forest stand age. Giscience and Remote Sensing 55 (3), 437–456. https://doi.org/10.1080/15481603.2017.1403136.

Dantas, V.d.L., Hirota, M., Oliveira, R.S., Pausas, J.G., Rejmanek, M., 2016. Disturbance maintains alternative biome states. Ecol. Lett. 19 (1), 12–19.

Davenport, M.L., Nicholson, S.E., 1993. On the relation between rainfall and the normalized difference vegetation index for diverse vegetation types in East Africa. Int. J. Remote Sens. 14 (12), 2369–2389. https://doi.org/10.1080/01431169308954042.

De Keersmaecker, W., Lhermitte, S., Hill, M.J., Tits, L., Coppin, P., Somers, B., 2017. Assessment of regional vegetation response to climate anomalies: a case study for Australia using GIMMS NDVI time series between 1982 and 2006. Remote Sens. (Basel) 9, 34. https://doi.org/10.3390/rs9010034.

de Souza, B.C., Carvalho, E.C.D., Oliveira, R.S., de Araújo, F.S., de Lima, A.L.A., Rodal, M.J.N., 2020. Drought response strategies of deciduous and evergreen woody species in a seasonally dry neotropical forest. Oecologia 194, 221–236. https://doi.org/10.1007/s00442-020-04760-3.

Dexter, K.G., Pennington, R.T., Oliveira-Filho, A.T., Bueno, M.L., Silva de Miranda, P.L., Neves, D.M., 2018. Inserting tropical dry forests into the discussion on biome transitions in the tropics. Front. Ecol. Evol. 6 (July), 1–7. https://doi.org/10.3389/fevo.2018.00104.

Dronova, I., Taddeo, S., 2022. Remote sensing of phenology: Towards the comprehensive indicators of plant community dynamics from species to regional scales. J. Ecol. 110 (7), 1460–1484.

Eamus, D., 1999. Ecophysiological traits of deciduous and evergreen woody species in the seasonally dry tropics,. ISSN 0169-5347 Trends in Ecology & Evolution 14 (1), 11–16. https://doi.org/10.1016/S0169-5347(98)01532-8.

El-Hokayem, L., De Vita, P., Conrad, C., 2023. Local identification of groundwater dependent vegetation using high-resolution Sentinel-2 data – a Mediterranean case study. Ecol. Ind. 146, 109784 https://doi.org/10.1016/j.ecolind.2022.109784.

Elias, F., Marimon Junior, B.H., de Oliveira, F.J.M., de Oliveira, J.C.A., Marimon, B.S., 2019. Soil and topographic variation as a key factor driving the distribution of tree flora in the Amazonia/Cerrado transition. Acta Oecol. 100, 103467 https://doi.org/10.1016/j.actao.2019.103467.

Emilio, T., Quesada, C.A., Costa, F.R.C., Magnusson, W.E., Schietti, J., Feldpausch, T.R., Brienen, R.J.W., Baker, T.R., Chave, J., Álvarez, E., Araújo, A., Bánki, O., Castilho, C. V., Honorio C., E.N., Killeen, T.J., Malhi, Y., Oblitas Mendoza, E.M., Monteagudo, A., Neill, D., Alexander Parada, G., Peña-Cruz, A., Ramirez-Angulo, H., Schwarz, M., Silveira, M., ter Steege, H., Terborgh, J.W., Thomas, R., Torres-Lezama, A., Vilanova, E., Phillips, O.L., 2014. Soil physical conditions limit palm and tree basal area in Amazonian forests. Plant Ecolog. Divers. 7 (1-2), 215–229.

Flores, B.M., de Sá Dechoum, M., Schmidt, I.B., Hirota, M., Abrahão, A., Verona, L., Pecoral, L.L.F., Cure, M.B., Giles, A.L., de Britto Costa, P., Pamplona, M.B., Mazzochini, G.G., Groenendijk, P., Minski, G.L., Wolfsdorf, G., Sampaio, A.B., Piccolo, F., Melo, L., Fiacador de Lima, R., Oliveira, R.S., Remy, C., 2021. Tropical riparian forests in danger from large savanna wildfires. J. Appl. Ecol. 58 (2), 419–430.

Funk, C., Peterson, P., Landsfeld, M., Pedreros, D., Verdin, J., Shukla, S., Husak, G., Rowland, J., Harrison, L., Hoell, A., Michaelsen, J., 2015. The climate hazards infrared precipitation with stations - a new environmental record for monitoring extremes. Sci. Data 2, 150066. https://doi.org/10.1038/sdata.2015.66.

Gao, X., McGregor, I.R., Gray, J.M., Friedl, M.A., Moon, M., 2023. Observations of satellite land surface phenology indicate that maximum leaf greenness is more associated with global vegetation productivity than growing season length. Global Biogeochem. Cycles 37. https://doi.org/10.1029/2022GB007462.

Goldstein, G., Rada, F., Rundel', P., Azocar, A., Orozco, A., 1989. Gas exchange and water relations of evergreen and deciduous tropical savanna trees. Ann. for. Sci. 46 (Supplement), 448s–453s.

Green, J.K., Berry, J., Ciais, P., Zhang, Y., Gentine, P., 2020. Amazon rainforest photosynthesis increases in response to atmospheric dryness. Science Advances 6 (47), eabb7232. https://doi.org/10.1126/sciadv.abb7232.

Guan, K., Pan, M., Li, H., Wolf, A., Wu, J., Medvigy, D., Caylor, K.K., Sheffield, J., Wood, E.F., Malhi, Y., Liang, M., Kimball, J.S., Saleska, S., Berry, J., Joiner, J., Lyapustin, A.I., 2015. Photosynthetic seasonality of global tropical forests constrained by hydroclimate. Nature Geosci 8 (4), 284–289.

Hansen, M.C., Potapov, P.V., Moore, R., Hancher, M., Turubanova, S.A., Tyukavina, A., Thau, D., Stehman, S.V., Goetz, S.J., Loveland, T.R., Kommareddy, A., Egorov, A., Chini, L., Justice, C.O., Townshend, J.R.G., 2013. High-resolution global maps of 21st-century forest cover change. Science 342 (6160), 850–853.

Hély, C., Bremond, L., Alleaume, S., Smith, B., Sykes, M.T., Guiot, J., 2006. Sensitivity of African biomes to changes in the precipitation regime. Glob. Ecol. Biogeogr. 15 (3), 258–270. https://doi.org/10.1111/J.1466-8238.2006.00235.X.

Hirota, M., Holmgren, M., van Nes, E.H., Scheffer, M., 2011. Global resilience of tropical forest and savanna to critical transitions. Science 334 (6053), 232–235. https://doi.org/10.1126/science.1210657.

Hoffmann, W.A., Geiger, E.L., Gotsch, S.G., Rossatto, D.R., Silva, L.C.R., Lau, O.L., Haridasan, M., Franco, A.C., Lloret, F., 2012. Ecological thresholds at the savanna-forest boundary: how plant traits, resources and fire govern the distribution of tropical biomes. Ecol. Lett. 15 (7), 759–768.

Ichii, K., Kawabata, A., Yamaguchi, Y., 2002. Global correlation analysis for NDVI and climatic variables and NDVI trends: 1982–1990. Int. J. Remote Sens. 23 (18), 3873–3878. https://doi.org/10.1080/01431160110119416.

Ishida, A., Diloksumpun, S., Ladpala, P., Staporn, D., Panuthai, S., Gamo, M., Yazaki, K., Ishizuka, M., Puangchit, L., 2006. Contrasting seasonal leaf habits of canopy trees between tropical dry-deciduous and evergreen forests in Thailand. Tree Physiol. 26 (5), 643–656. https://doi.org/10.1093/treephys/26.5.643.

Jiang, Z., Huete, A.R., Didan, K., Miura, T., 2008. Development of a two-band enhanced vegetation index without a blue band. Remote Sens. Environ. 112 (10), 3833–3845. https://doi.org/10.1016/j.rse.2008.06.006.

Kellman, M., Meave, J., 1997. Fire in the tropical gallery forests of Belize. J. Biogeogr. 24 (1), 23–34. https://doi.org/10.1111/j.1365-2699.1997.tb00047.x.

Kikuzawa, K., 1995. The basis for variation in leaf longevity of plants. Vegetatio 121 (1-2), 89–100.

Lawes, M.J., Richards, A., Dathe, J., Midgley, J.J., 2011. Bark thickness determines fire resistance of selected tree species from fire-prone tropical savanna in north Australia. Plant Ecol 212 (12), 2057–2069.

Lawes, M.J., Midgley, J.J., Clarke, P.J., Jones, R., 2013. Costs and benefits of relative bark thickness in relation to fire damage: a savanna/forest contrast. J. Ecol. 101 (2), 517–524.

Lee, E., Kumar, P., Knowles, J.F., Minor, R.L., Tran, N., Barron-Gafford, G.A., Scott, R.L., 2021. Convergent hydraulic redistribution and groundwater access supported facilitative dependency between trees and grasses in a semi-arid environment. Water Resour. Res. 57 (6) https://doi.org/10.1029/2020WR028103.

Lehmann, C.E.R., Anderson, T.M., Sankaran, M., Higgins, S.I., Archibald, S., Hoffmann, W.A., Hanan, N.P., Williams, R.J., Fensham, R.J., Felfili, J., Hutley, L.B., Ratnam, J., San Jose, J., Montes, R., Franklin, D., Russell-Smith, J., Ryan, C.M., Durigan, G., Hiernaux, P., Haidar, R., Bowman, D.M.J.S., Bond, W.J., 2014. Savanna vegetation-fire-climate relationships differ among continents. Science 343 (6170), 548–552.

Lenth, R.V., 2022. emmeans: Estimated Marginal Means, aka Least-Squares Means. R Package Version 1.7.4-1. https://CRAN.R-project.org/package=emmeans.

Liang, J., Crowther, T.W., Picard, N., Wiser, S., Zhou, M., Alberti, G., Schulze, E.D., McGuire, A.D., Bozzato, F., Pretzsch, H., De-Miguel, S., Paquette, A., Hérault, B., Scherer-Lorenzen, M., Barrett, C.B., Glick, H.B., Hengeveld, G.M., Nabuurs, G.J., Pfautsch, S., Reich, P.B., 2016. Positive biodiversity-productivity relationship predominant in global forests. Science 354 (6309). https://doi.org/10.1126/science.aaf8957.

Lira-Martins, D., Nascimento, D.L., Abrahão, A., de Britto Costa, P., D'Angioli, A.M., Valézio, E., Rowland, L., Oliveira, R.S., 2022. Soil properties and geomorphic processes influence vegetation composition, structure, and function in the Cerrado Domain. Plant and Soil 476 (1-2), 549–588.

Liu, H., Gleason, S.M., Hao, G., Hua, L., He, P., Goldstein, G., Ye, Q., 2019. Hydraulic traits are coordinated with maximum plant height at the global scale. Science Advances 5 (2). https://doi.org/10.1126/SCIADV.AAV1332/.

Lohbeck, M., Poorter, L., Lebrija-Trejos, E., Martínez-Ramos, M., Meave, J.A., Paz, H., Pérez-García, E.A., Romero-Pérez, I.E., Tauro, A., Bongers, F., 2013. Successional changes in functional composition contrast for dry and wet tropical forest. Ecology 94, 1211–1216. https://doi.org/10.1890/12-1850.1.

Lopes, A.S., Cox, F.R., 1977. Cerrado Vegetation in Brazil: An Edaphic Gradient. Agron. J. 69, 828–831. https://doi.org/10.2134/agronj1977.00021962006900050025x.

Loram-Lourenço, L., Farnese, F.S., Alves, R.D.F.B., Dario, B.M.M., Martins, A.C., Aun, M. A., Batista, P.F., Silva, F.G., Cochard, H., Franco, A.C., Menezes-Silva, P.E., 2022. Variations in bark structural properties affect both water loss and carbon economics

in neotropical savanna trees in the Cerrado region of Brazil. J. Ecol. 110 (8), 1826–1843.
Lotsch, A., Friedl, M.A., Anderson, B.T., Tucker, C.J., 2003. Coupled vegetation-precipitation variability observed from satellite and climate records. Geophys. Res. Lett. 30, 1774. https://doi.org/10.1029/2003GL017506.
Ma, X., Huete, A., Moore, C.E., Cleverly, J., Hutley, L.B., Beringer, J., Leng, S., Xie, Z., Yu, Q., Eamus, D., 2020. Spatiotemporal partitioning of savanna plant functional type productivity along NATT. Remote Sens. Environ. 246, 111855 https://doi.org/10.1016/j.rse.2020.111855.
Maestre, F.T., Eldridge, D.J., Soliveres, S., Kéfi, S., Delgado-Baquerizo, M., Bowker, M.A., García-Palacios, P., Gaitán, J., Gallardo, A., Lázaro, R., Berdugo, M., 2016. Structure and functioning of dryland ecosystems in a changing world. Annu. Rev. Ecol. Evol. Syst. 47, 215–237. https://doi.org/10.1146/ANNUREV-ECOLSYS-121415-032311.
Maksic, J., Venancio, I.M., Shimizu, M.H., Chiessi, C.M., Piacsek, P., Sampaio, G., Cruz, F.W., Alexandre, F.F., 2022. Brazilian biomes distribution: past and future. Palaeogeogr. Palaeoclimatol. Palaeoecol. 585, 110717 https://doi.org/10.1016/J.PALAEO.2021.110717.
Projeto MapBiomas - Collection 7 of the Annual Series of Land Use and Land Cover Maps of Brazil, accessed on April 08, 2022, via the link: https://mapbiomas.org.
Maracahipes, L., Carlucci, M.B., Lenza, E., Marimon, B.S., Marimon, B.H., Guimarães, F. A.G., Cianciaruso, M., v., 2018. How to live in contrasting habitats? Acquisitive and conservative strategies emerge at inter- and intraspecific levels in savanna and forest woody plants. Perspectives in Plant Ecology, Evolution and Systematics 34, 17–25. https://doi.org/10.1016/j.ppees.2018.07.006.
Markham, C.G., 1970. Seasonality of precipitation in the United States. Ann. Assoc. Am. Geogr. 60 (3), 593–597. https://doi.org/10.1111/J.1467-8306.1970.TB00743.X.
Mattos, C.R., Hirota, M., Oliveira, R.S., Flores, B.M., Miguez-Macho, G., Pokhrel, Y., Fan, Y., 2023. Double stress of waterlogging and drought drives forest–savanna coexistence. Proc. Natl. Acad. Sci. 120 (33) https://doi.org/10.1073/pnas.2301255120.
Mazzochini, G.G., Fonseca, C.R., Costa, G.C., Santos, R.M., Oliveira-Filho, A.T., Ganade, G., Mayfield, M., 2019. Plant phylogenetic diversity stabilizes large-scale ecosystem productivity. Glob. Ecol. Biogeogr. 28 (10), 1430–1439.
McDowell, N., Barnard, H., Bond, B.J., Hinckley, T., Hubbard, R.M., Ishii, H., Köstner, B., Magnani, F., Marshall, J.D., Meinzer, F.C., Phillips, N., Ryan, M.G., Whitehead, D., 2002. The relationship between tree height and leaf area: Sapwood area ratio. Oecologia 132, 12–20. https://doi.org/10.1007/S00442-002-0904-X.
McLeod, A. I. (2011). *Kendall rank correlation and Mann-Kendall trend test* (2.2). https://cran.r-project.org/web/packages/Kendall/Kendall.pdf.
McNaughton, S.J., Oesterheld, M., Frank, D.A., Williams, K.J., 1989. Ecosystem-level patterns of primary productivity and herbivory in terrestrial habitats. Nature 341, 142–144. https://doi.org/10.1038/341142a0.
Metzen, D., Sheridan, G., Benyon, R., Bolstad, P.V., Griebel, A., Lane, P.N.J., 2019. Spatio-temporal transpiration patterns reflect vegetation structure in complex upland terrain. Sci. Total Environ. 694, 133551 https://doi.org/10.1016/j.scitotenv.2019.07.357.
Michaletz, S.T., Cheng, D., Kerkhoff, A.J., Enquist, B.J., 2014. Convergence of terrestrial plant production across global climate gradients. Nature 512 (7512), 39–43.
Migliavacca, M., Musavi, T., Mahecha, M.D., Nelson, J.A., Knauer, J., Baldocchi, D.D., Perez-Priego, O., Christiansen, R., Peters, J., Anderson, K., Bahn, M., Black, T.A., Blanken, P.D., Bonal, D., Buchmann, N., Caldararu, S., Carrara, A., Carvalhais, N., Cescatti, A., Chen, J., Cleverly, J., Cremonese, E., Desai, A.R., El-Madany, T.S., Farella, M.M., Fernández-Martínez, M., Filippa, G., Forkel, M., Galvagno, M., Gomarasca, U., Gough, C.M., Göckede, M., Ibrom, A., Ikawa, H., Janssens, I.A., Jung, M., Kattge, J., Keenan, T.F., Knohl, A., Kobayashi, H., Kraemer, G., Law, B.E., Liddell, M.J., Ma, X., Mammarella, I., Martini, D., Macfarlane, C., Matteucci, G., Montagnani, L., Pabon-Moreno, D.E., Panigada, C., Papale, D., Pendall, E., Penuelas, J., Phillips, R.P., Reich, P.B., Rossini, M., Rotenberg, E., Scott, R.L., Stahl, C., Weber, U., Wohlfahrt, G., Wolf, S., Wright, I.J., Yakir, D., Zaehle, S., Reichstein, M., 2021. The three major axes of terrestrial ecosystem function. Nature 598 (7881), 468–472.
Moeslund, J.E., Arge, L., Bøcher, P.K., Dalgaard, T., Odgaard, M.V., Nygaard, B., Svenning, J.-C., 2013. Topographically controlled soil moisture is the primary driver of local vegetation patterns across a lowland region. Ecosphere 4 (7), art91. https://doi.org/10.1890/ES13-00134.1.
Monteith, J.L., 1972. Solar radiation and productivity in tropical ecosystems. J. Appl. Ecol. 9 (3), 747–766. https://doi.org/10.2307/2401901.
Murphy, B.P., Bowman, D.M.J.S., 2012. What controls the distribution of tropical forest and savanna? Ecol. Lett. 15 (7), 748–758. https://doi.org/10.1111/j.1461-0248.2012.01771.x.
Murtagh, F., Legendre, P., 2014. Ward's hierarchical agglomerative clustering method: which algorithms implement Ward's criterion? J. Classif. 31, 274–295. https://doi.org/10.1007/s00357-014-9161-z.
Oehri, J., Schmid, B., Schaepman-Strub, G., Niklaus, P.A., 2017. Biodiversity promotes primary productivity and growing season lengthening at the landscape scale. Proc. Natl. Acad. Sci. 114 (38), 10160–10165. https://doi.org/10.1073/pnas.1703928114.
Oksanen, J., Blanchet, F. G., Friendly, M., Kindt, R., Legendre, P., McGlinn, D., Minchin, P., O'Hara, R., Simpson, G., Solymos, P., Stevens, M., Szöcs, E., & Wagner, H. (2020). *Vegan community ecology package version 2.5-7 november 2020*.
Oliveira, R.S., Bezerra, L., Davidson, E.A., Pinto, F., Klink, C.A., Nepstad, D.C., Moreira, A., 2005. Deep root function in soil water dynamics in cerrado savannas of central brazil. Funct. Ecol. 19 (4), 574–581. https://doi.org/10.1111/j.1365-2435.2005.01003.x.
Oliveira, R.S., Eller, C.B., Barros, F.d.V., Hirota, M., Brum, M., Bittencourt, P., 2021. Linking plant hydraulics and the fast-slow continuum to understand resilience to drought in tropical ecosystems. New Phytol. 230 (3), 904–923.
Oliveira, P.S., Marquis, R.J., 2002. The Cerrados of Brazil: Ecology and Natural History of a Neotropical Savanna. Columbia University Press, p. 398 p..
Paula, G.A., Fischer, E., Silveira, M., Almeida, H., van den Berg, E., 2023. Woody species distribution across a savanna-dry forest soil gradient in the Brazilian Cerrado/Distribuição de espécies arbóreas em gradiente de solo savana-floresta seca no Cerrado brasileiro. Braz. J. Biol. 83 https://doi.org/10.1590/1519-6984.243245.
Pausas, J.G., Bond, W.J., 2021. Alternative biome states challenge the modelling of species' niche shifts under climate change. J. Ecol. 109 (12), 3962–3971. https://doi.org/10.1111/1365-2745.13781.
Pausas, J.G., Poorter, L., 2015. Bark thickness and fire regime. Funct. Ecol. 29 (3), 315–327.
Pennington, R.T., Lehmann, C.E.R., Rowland, L.M., 2018. Tropical savannas and dry forests. Curr. Biol. 28 (9), R541–R545. https://doi.org/10.1016/j.cub.2018.03.014.
Priyadarshini, K.V.R., Prins, H.H.T., de Bie, S., Heitkönig, I.M.A., Woodborne, S., Gort, G., Kirkman, K., Ludwig, F., Dawson, T.E., de Kroon, H., 2016. Seasonality of hydraulic redistribution by trees to grasses and changes in their water-source use that change tree – grass interactions. Ecohydrology 9, 218–228. https://doi.org/10.1002/eco.1624.
R Core Team. (2021). *R: A language and environment for statistical computing*. R Foundation for Statistical Computing. https://www.R-project.org/.
Ratter, J.A., Dargie, T.C.D., 1992. An analysis of the floristic composition of 26 Cerrado areas in Brazil. Edinb. J. Bot., Edinburgh 49 (2), 235–250.
Ribeiro, J. F., & Walter, B. M. T. (2008). As principais fitofisionomias do bioma Cerrado. In *Cerrado: Ecologia e Flora* (1st ed., Vol. 1, pp. 151–212).
Ribeiro, J.F., Sano, S.M., Macedo, J., da Silva, J.A., 1983. Os principais tipos fitofisionomicos da regiao dos cerrados. EMBRAPA - CPAC. https://www.embrapa.br/busca-de-publicacoes/-/publicacao/548930/os-principais-tipos-fitofisionomicos-da-regiao-dos-cerrados.
Rosell, J.A., 2019. Bark in woody plants: understanding the diversity of a multifunctional structure. Integr. Comp. Biol. 59 (3), 535–547. https://doi.org/10.1093/ICB/ICZ057.
Rozendaal, D.M.A., Phillips, O.L., Lewis, S.L., Affum-Baffoe, K., Alvarez-Davila, E., Andrade, A., Aragão, L.E.O.C., Araujo-Murakami, A., Baker, T.R., Bánki, O., Brienen, R.J.W., Camargo, J.L.C., Comiskey, J.A., Djuikouo Kamdem, M.N., Fauset, S., Feldpausch, T.R., Killeen, T.J., Laurance, W.F., Laurance, S.G.W., Lovejoy, T., Malhi, Y., Marimon, B.S., Marimon Junior, B.-H., Marshall, A.R., Neill, D.A., Núñez Vargas, P., Pitman, N.C.A., Poorter, L., Reitsma, J., Silveira, M., Sonké, B., Sunderland, T., Taedoumg, H., ter Steege, H., Terborgh, J.W., Umetsu, R. K., van der Heijden, G.M.F., Vilanova, E., Vos, V., White, L.J.T., Willcock, S., Zemagho, L., Vanderwel, M.C., 2020. Competition influences tree growth, but not mortality, across environmental gradients in Amazonia and tropical Africa. Ecology 101 (7). https://doi.org/10.1002/ECY.3052.
Ryan, M.G., Yoder, B.J., 1997. Hydraulic limits to tree height and tree growth: What keeps trees from growing beyond a certain height? Bioscience 47 (4), 235–242. https://doi.org/10.2307/1313077.
Saleska, S.R., Didan, K., Huete, A.R., da Rocha, H.R., 2007. Amazon forests green-up during 2005 drought. Science 318 (5850), 612.
Santos, P., Negri, A.J., 1997. A comparison of the normalized difference vegetation index and rainfall for the Amazon and Northeastern Brazil. Journal of Applied Meteorology Climatology 36, 958–965. https://doi.org/10.1175/1520-0450(1997)036%3C0958:ACOTND%3E2.0.CO;2.
Scheffer, M., Carpenter, S., Foley, J.A., Folke, C., Walker, B., 2001. Catastrophic shifts in ecosystems. Nature 413 (6856), 591–596.
Schmidt, H., Karnieli, A., 2000. Remote sensing of the seasonal variability of vegetation in a semi-arid environment. J. Arid Environ. 45 (1), 43–59. https://doi.org/10.1006/jare.1999.0607.
Scholz, F.G., Bucci, S.J., Goldstein, G., Moreira, M.Z., Meinzer, F.C., Domec, J.C., Villalobos-Vega, R., Franco, A.C., Miralles-Wilhelm, F., 2008. Biophysical and life-history determinants of hydraulic lift in Neotropical savanna trees. Funct. Ecol. 22 (5), 773–786. https://doi.org/10.1111/J.1365-2435.2008.01452.X.
Sijtsma, K., Emons, W.H.M. (2010). Nonparametric Statistical Methods. in: Peterson, P., Baker, E., McGaw, B. (Eds). International Encyclopedia of Education (Third Edition), Elsevier, pp. 347-353, ISBN 9780080448947. https://doi.org/10.1016/B978-0-08-044894-7.01353-1.
Silva, J.F., Farinas, M.R., Felfili, J.M., Klink, C.A., 2006. Spatial heterogeneity, land use and conservation in the cerrado region of Brazil. J. Biogeogr. 33 (3), 536–548. https://doi.org/10.1111/j.1365-2699.2005.01422.x.
Simon, M.F., Grether, R., de Queiroz, L.P., Skema, C., Pennington, R.T., Hughes, C.E., 2009. Recent assembly of the Cerrado, a neotropical plant diversity hotspot, by in situ evolution of adaptations to fire. Proc. Natl. Acad. Sci. 106 (48), 20359–20364. https://doi.org/10.1073/PNAS.0903410106.
Simon, M.F., Pennington, T., 2012. evidence for adaptation to fire regimes in the tropical savannas of the Brazilian Cerrado. Int. J. Plant Sci. 173 (6), 711–723. https://doi.org/10.1086/665973.
Slik, J.W.F., Aiba, S.-I., Brearley, F.Q., Cannon, C.H., Forshed, O., Kitayama, K., Nagamasu, H., Nilus, R., Payne, J., Paoli, G., Poulsen, A.D., Raes, N., Sheil, D., Sidiyasa, K., Suzuki, E., van Valkenburg, J.L.C.H., 2010. Environmental correlates of tree biomass, basal area, wood specific gravity and stem density gradients in Borneo's tropical forests. Glob. Ecol. Biogeogr. 19 (1), 50–60.
Smith, M.N., Taylor, T.C., van Haren, J., Rosolem, R., Restrepo-Coupe, N., Adams, J., Wu, J., de Oliveira, R.C., da Silva, R., de Araujo, A.C., de Camargo, P.B., Huxman, T. E., Saleska, S.R., 2020. Empirical evidence for resilience of tropical forest

photosynthesis in a warmer world. Nat. Plants 6 (10), 1225–1230. https://doi.org/10.1038/s41477-020-00780-2.

Sobrado, M.A., 1991. Cost-benefit relationships in deciduous and evergreen leaves of tropical dry forest species. Funct. Ecol. 5 (5), 616. https://doi.org/10.2307/2389479.

Souza, C.M., Z. Shimbo, J., Rosa, M.R., Parente, L.L., A. Alencar, A., Rudorff, B.F.T., Hasenack, H., Matsumoto, M., G. Ferreira, L., Souza-Filho, P.W.M., de Oliveira, S.W., Rocha, W.F., Fonseca, A.V., Marques, C.B., Diniz, C.G., Costa, D., Monteiro, D., Rosa, E.R., Vélez-Martin, E., Weber, E.J., Lenti, F.E.B., Paternost, F.F., Pareyn, F.G. C., Siqueira, J.V., Viera, J.L., Neto, L.C.F., Saraiva, M.M., Sales, M.H., Salgado, M.P. G., Vasconcelos, R., Galano, S., Mesquita, V.V., Azevedo, T., 2020. Reconstructing Three Decades of Land Use and Land Cover Changes in Brazilian Biomes with Landsat Archive and Earth Engine. Remote Sens. (Basel) 12 (17), 2735.

Staal, A., & Flores, B. M. (2015). Sharp ecotones spark sharp ideas: comment on "Structural, physiognomic and above-ground biomass variation in savanna-forest transition zones on three continents-how different are co-occurring savanna and forest formations?" by Veenendaal et al. (2015). *Biogeosciences*, *12*, 5563–5566. https://doi.org/10.5194/bg-12-5563-2015.

Staver, A.C., Archibald, S., Levin, S.A., 2011. The global extent and determinants of savanna and forest as alternative biome states. Science 334 (6053), 230–232.

Turner, M.G., Chapin, F.S., 2005. Causes and Consequences of Spatial Heterogeneity in Ecosystem Function. In: Lovett, G.M., Turner, M.G., Jones, C.G., Weathers, K.C. (Eds.), Ecosystem Function in Heterogeneous Landscapes. Springer New York, New York, NY, pp. 9–30.

Veenendaal, E.M., Torello-Raventos, M., Feldpausch, T.R., Domingues, T.F., Gerard, F., Schrodt, F., Saiz, G., Quesada, C.A., Djagbletey, G., Ford, A., Kemp, J., Marimon, B. S., Marimon-Junior, B.H., Lenza, E., Ratter, J.A., Maracahipes, L., Sasaki, D., Sonké, B., Zapfack, L., Villarroel, D., Schwarz, M., Yoko Ishida, F., Gilpin, M., Nardoto, G.B., Affum-Baffoe, K., Arroyo, L., Bloomfield, K., Ceca, G., Compaore, H., Davies, K., Diallo, A., Fyllas, N.M., Gignoux, J., Hien, F., Johnson, M., Mougin, E., Hiernaux, P., Killeen, T., Metcalfe, D., Miranda, H.S., Steininger, M., Sykora, K., Bird, M.I., Grace, J., Lewis, S., Phillips, O.L., Lloyd, J., 2015. Structural, physiognomic and above-ground biomass variation in savanna-forest transition zones on three continents-how different are co-occurring savanna and forest formations? Biogeosciences 12 (10), 2927–2951.

Veenendaal, E.M., Torello-Raventos, M., Miranda, H.S., Sato, N.M., Oliveras, I., van Langevelde, F., Asner, G.P., Lloyd, J., 2018. On the relationship between fire regime and vegetation structure in the tropics. New Phytol. 218 (1), 153–166. https://doi.org/10.1111/nph.14940.

Veneklaas, E.J., Fajardo, A., Obregon, S., Lozano, J., 2005. Gallery forest types and their environmental correlates in a Colombian savanna landscape. Ecography 28 (2), 236–252. https://doi.org/10.1111/J.0906-7590.2005.03934.X.

Wang, J., Rich, P.M., Price, K.P., 2003. Temporal responses of NDVI to precipitation and temperature in the central Great Plains, USA. Int. J. Remote Sens. 24 (11), 2345–2364. https://doi.org/10.1080/01431160210154812.

Western, A.W., Grayson, R.B., Blöschl, G., Willgoose, G.R., McMahon, T.A., 1999. Observed spatial organization of soil moisture and its relation to terrain indices. Water Resour. Res. 35 (3), 797–810. https://doi.org/10.1029/1998WR900065.

Whitecross, M.A., Witkowski, E.T.F., Archibald, S., 2017. Savanna tree-grass interactions: a phenological investigation of green-up in relation to water availability over three seasons. S. Afr. J. Bot. 108, 29–40. https://doi.org/10.1016/j.sajb.2016.09.003.

Xu, C., Hantson, S., Holmgren, M., van Nes, E.H., Staal, A., Scheffer, M., 2016. Remotely Sensed Canopy Height Reveals Three Pantropical Ecosystem States. 97 (9), 2518–2521.

Yamazaki, D., Ikeshima, D., Sosa, J., Bates, P.D., Allen, G.H., Pavelsky, T.M., 2019. MERIT hydro: A high-resolution global hydrography map based on latest topography dataset. Water Resour. Res. 55 (6), 5053–5073. https://doi.org/10.1029/2019WR024873.

Seddon, A. W. R., Macias-Fauria, M., Long, P. R., Benz, D., & Willis, K. J. (2016). Sensitivity of global terrestrial ecosystems to climate variability. *Nature 2016 531: 7593*, *531*(7593), 229–232. https://doi.org/10.1038/nature16986.

van Nes EH, Staal A, Hantson S, Holmgren M, Pueyo S, Bernardi RE, Flores BM, Xu C, Scheffer M. Fire forbids fifty-fifty forest. PLoS One. 2018 Jan 19;13(1):e0191027. doi: 10.1371/journal.pone.0191027.

Soares Jancoski, H., Schwantes Marimon, B., C. Scalon, M., de V. Barros, F., Marimon-Junior, B. H., Carvalho, E., S. Oliveira, R., & Oliveras Menor, I. (2022). Distinct leaf water potential regulation of tree species and vegetation types across the Cerrado–Amazonia transition. *Biotropica*, *54*(2), 431–443. https://doi.org/10.1111/BTP.13064.

Further reading

Projeto MapBiomas – Fire Scars Mapping in Brazil Collection 1, accessed on October 08, 2021, through the link: https://code.earthengine.google.com/?scriptPath=users%2Fmapbiomas%2Fuser-toolkit%3Amapbiomas-user-toolkit-fire.js.